

## Recrystallized RGTi Graphite Application as the First Wall Material in Globus-M Spherical Tokamak

V.K. Gusev<sup>1</sup>, V.Kh. Alimov<sup>2</sup>, I.I. Arkhipov<sup>2</sup>, M. Balden<sup>3</sup>, E.A. Denisov<sup>4</sup>, A.E. Gorodetsky<sup>2</sup>, A.A. Kurdumov<sup>4</sup>, T.N. Kompaniec<sup>4</sup>, V.M. Lebedev<sup>5</sup>, N.V. Litunovskii<sup>6</sup>, I.V. Mazul<sup>6</sup>, A.N. Novokhatsky<sup>1</sup>, Yu.V. Petrov<sup>1</sup>, N.V. Sakharov<sup>1</sup>, V.M. Sharapov<sup>2</sup>, E.I. Terukov<sup>1</sup>, I.N. Trapeznikova<sup>1</sup>, J. Roth<sup>3</sup>, A.P. Zakharov<sup>2</sup>, R.Kh. Zalavutdinov<sup>2</sup>

<sup>1</sup> A.F.Ioffe Physico-Technical Institute, Russian Academy of Science, St.Petersburg, Russia

<sup>2</sup> Institute of Physical Chemistry and Electrochemistry, Russian Academy of Sciences, Moscow, Russia

<sup>3</sup> Max-Planck-Institut für Plasmaphysik, EURATOM Association, Garching, Germany

<sup>4</sup> Research Institute of Physics of St. Petersburg State University, St.Petersburg, Russia

<sup>5</sup> B.P.Konstantinov Nuclear Physics Institute, Russian Academy of Science, Gatchina, Russia

<sup>6</sup> D.V.Efremov Institute of Electrophysical Apparatus, St.Petersburg, Russia

PACS Codes: 52.40.Hf, 52.55.Fa

Keywords: spherical tokamak, RGTi graphite tiles, mixed layers, deuterium retention

### Abstract

Recrystallized RGTi graphite tiles were extracted from the first wall of the Globus-M spherical tokamak after being used as plasma-facing components (PFCs) during more than 8000 pulses (more than 800 s). The analysis of chemical composition and structure of the irradiated tiles was performed by different methods. It was found that most of the tiles were covered with mixed layers. In the deposits the amount of absorbed deuterium was measured and minimum D concentration was found in the region of maximum power loads. Only a small amount of deuterium has been detected in the bulk of RGTi tiles exposed to plasma.

### 1. Introduction

Globus-M is the first Russian spherical tokamak built at A.F.Ioffe Physico-Technical Institute in 1999. It can operate with high plasma density up to  $10^{20} \text{ m}^{-3}$  and high specific power deposition into the plasma volume up to a few  $\text{MW/m}^3$  [1]. Tiny plasma-wall spacing and small ratio of the first wall area to plasma volume result in large power density loads to the first wall. Almost 90% of the inner vacuum vessel (austenitic stainless steel) surface area, which is directly faced to plasma, is now covered by RGTi tiles doped with 2 at.% Ti and 0.3-0.7 at.% Si, see Table 1, Fig. 1, [2, 3]. A constant plasma performance improvement was observed alongside with increased RGTi tiles area. The PFCs were protected by B/C:H films [4] using 7-8 procedures of boronization per year (20-30 in total). Fig. 2 shows divertor plasma configuration (poloidal cross-section of plasma equilibrium magnetic surfaces). The direction of main power fluxes to target PFCs in the region of open magnetic field lines called scrape-off-layer (SOL) are shown by the arrows. According to power fluxes distribution in spherical tokamaks [5], one could expect about 70-90% of power and charged particle fluxes in SOL are directed towards the area of the outer divertor targets (toroidal belts covered by the tiles 1 and 2 in Figs. 1 and 2). During each Globus-M

discharge between 0.5 and 1 MW of power is launched into plasma and significant part of it is deposited onto the outer target PFCs area of  $\sim 0.5 \text{ m}^2$ . On the other hand the power loads to the inner target PFCs (tiles 5, 6) is much less (4-30 times). Tiles 3 and 4 are in the intermediate zone of even lower power loads placed between separatrix “legs”. PFC tiles 7 and 8 miss main power flux in SOL, which is parallel to their surface.

The goal of the paper is to analyze the composition of surface deposits on RGTi tiles (with respect to reference tile 9, which was not installed in the device) after irradiation of tiles 1-8 by Globus-M plasma during significant period of time (8000-12000 discharges, 800 – 1000 s total duration).

## 2. Analysis Techniques

The samples for analyses were cut out from the middle of tiles 1-8 and reference tile 9. For determining the D concentration in the bulk, a surface layer of  $\sim 100 \mu\text{m}$  was removed by grinding.

Composition and morphology of the sample surface layers were examined by electron probe microanalysis (EPMA) with energy dispersive (EDX) and wavelength dispersive (WDX) X-ray spectrometers using a 5-30 keV electron beam [6] and by scanning electron microscope (SEM with EDX, FEI, XL30-ESEM). In addition, composition was analyzed by Rutherford backscattering (RBS) [7].

Deuterium depth profiles were determined by the  $D(^3\text{He},p)^4\text{He}$  nuclear reaction in a resonance-like technique (NRA) [8]. To determine the D depth distribution, an analyzing beam of  $^3\text{He}$  ions with energies varied from 0.69 to 3.2 MeV was used. D concentration profile in deeper layers was obtained with the computer program SIMNRA [9] by deconvoluting the proton yields measured at different  $^3\text{He}$  ion energies.

Additionally, the integral deuterium retention in tiles was studied by thermal desorption spectroscopy (TDS) with using an electron impact for heating [10]. The heating rate was 3.2 K/s. The releasing of  $\text{D}_2$  and HD molecules was controlled by a quadrupole mass spectrometer. An average value of the  $\text{H}_2$  and  $\text{D}_2$  sensitivities was accepted as the sensitivity for HD molecules [10]. The structure of near-surface layers (up to 10  $\mu\text{m}$  thickness) was studied with X-ray diffraction technique (XRD) at angles of  $2\theta = 20\text{-}90^\circ$  using  $\text{CuK}_\alpha$  radiation.

## 3. Results

The XRD analysis has shown that all samples have a distinct texture with basal plane (002) parallel to the vacuum vessel surface. It has a well-ordered three-dimensional structure (Table 1, interplanar spacing, crystallite size). The precipitates of TiC cubic carbide with sizes of 0.3-3  $\mu\text{m}$  have a tendency to locate

with (200) TiC face in parallel to (002) graphite plane. The observed texture is correlated to the uniaxial pressing during the production of the material (perpendicular to surface) [2].

The deposition of the metallic elements of vacuum vessel and in-vessel components together with carbon and boron took place on samples 1-6 (Fig. 3, a-c and Table 2). Samples 7 and 8 were subjected to erosion and destruction (Fig. 3, d) and only very low deposition. From XRD data of the samples 7 and 8, it followed that the primary orientation of graphite was lost and that blocks of graphite of a few  $\mu\text{m}$  size were turned to an arbitrary angle. In this destroyed layer the titanium carbide content was increased compared to sample 9.

Samples 1-6 were covered with deposits consisting of carbon, oxygen, titanium and impurities (Table 2).

In the EDX measurements with 5-30 keV beam it was observed that deposited layer on sample 3 contained carbon atoms in amount comparable with boron atoms. The same conclusion follows from EDX studies of samples 1, 2, 4-6 using 15 keV beam. The most deposition of boron and carbon occurred on samples 3 and 4. If we assume that B/C deposit density is  $5 \times 10^{22}$  at./ $\text{cm}^3$ , the deposit thicknesses will be 2.6  $\mu\text{m}$ . Besides boron and carbon the deposits contained practically all elements of constructional materials, which were in line-of-sight with the plasma. The distribution of metals on samples 1-6 was more uniform than of boron one. The tendency to higher metal deposition was observed on samples 3-6.

Besides the elements mentioned above, the deposits contained oxygen and deuterium (Fig. 4). The increased O concentration in the near-surface layer may be connected with additional oxidation of deposits in air.

The deuterium concentration in mixed layers was below 8 at.%. The deuterium content in mixed layers increases with sample number. Significantly lower deuterium content was measured in samples 7 and 8 (Table 3, NRA data). TDS measurements confirmed the general tendency of increasing D content with sample number and demonstrated that D concentration in RGTi bulk (after removing of 100  $\mu\text{m}$  surface layer) turned out to be about  $2 \times 10^{-3}$  at.%. The maximal rate of HD and D<sub>2</sub> molecules release occurred at 600-900 K that was significantly lower than in the case of deuterium release from RGTi bulk [10]. This indicates predominant retention of deuterium in deposits.

#### **4. Conclusions**

It has been shown that the PFC tiles 7 and 8 oriented vertically are subjected to erosion and destruction.

They missed main power and ionized particle fluxes focused at divertor tiles 1-6. The reason of destruction may be in the periodical contact with expanding plasma column during initial phase of the discharge and/or in the bombardment by energetic neutral particles (tens of keV energy) as the distance between vertically oriented tiles and hot plasma body is short. The tiles 1-6 were covered with deposits

(mixed layers) of different elements. Thicker mixed layers occurred on tiles 3-6, as observed by EPMA method. Deuterium retention in mixed layers exhibited weak correlation with the layer thickness. The amount of absorbed deuterium increases with increasing tile number (1-6), demonstrating a minimum in the zone of maximum power load (tiles 1 and 2). In the bulk of RGTi tiles (underneath the mixed layers), a small amount of the retained deuterium has been detected.

#### **Acknowledgement**

The work is supported by Rosnauka RF and RFBR grants ## 05-08-18044, 06-02-16709, 06-02-08186, 06-03-32854, 06-08-00878, 07-02-13557.

#### **References**

- [1] V.K. Gusev et al., Technical Physics 44 (1999) 1054.
- [2] T.A. Burtseva et al., Carbon Materials, Proceedings of 6th International Workshop, Jülich, Germany, 23-24 September, 1993, 49.
- [3] A.E. Gorodetsky et al., Fus. Eng. Des. 43 (1998) 129.
- [4] V.M. Sharapov et al., J. Nucl. Mater. 220-222 (1995) 730.
- [5] G.F. Counsell et al., Nucl. Fusion 43 (2003) 1197.
- [6] R.Kh. Zalavutdinov et al., Microchim. Acta 114-115 (1994) 533.
- [7] J.R. Tesmer et al., Handbook of Modern Ion Beam Materials Analysis (Materials Research Society, Pittsburgh, Pa., USA, 1995).
- [8] V.Kh. Alimov et al., Nucl. Instr. and Meth. B 234 (2005) 169.
- [9] M. Mayer, SIMNRA User's Guide, Tech. Rep. IPP 9/113, Garching, 1997, and [www.rzg.mpg.de/~mam](http://www.rzg.mpg.de/~mam).
- [10] I.I. Arkhipov et al., J. Nucl. Mater. 271-272 (1999) 418.

## Figure captions

Fig.1. Divertor RGTi tiles assembled inside Globus-M vacuum vessel.

Fig.2. Divertor configuration and equilibrium plasma magnetic surfaces.

Fig. 3. SEM micrographs of the RGTi surfaces exposed to D plasma. Samples: 2 – (a); 4 – (b); 5 – (c); 8 – (d) magnified higher than (a) – (c).

Fig. 4. Elemental depth distributions in sample 6 as determined from the RBS and NRA spectra. Label Me indicates the integral concentration of metals Ti, Cr, Fe, Ni, Cu.

**Table 1.** Parameters of RGTi and graphite single crystal (GSC). GSC data are from Russian handbook on graphite crystals. RGTi data are from [2]

Material	RGTi	GSC
Density, g/cm <sup>3</sup>	2.24-2.26	2.267
Porosity, vol. %	0.2-0.5	0
Thermal conductivity at 400 K in [002]/[100] directions, W/m K	100/500	≈100/1000
Interplanar spacing in [002]/[100] directions, nm	0.3357// 0.2132	0.3354// 0.2131
Graphite crystallite size, μm	1-10	100

**Table 2.** Partial thicknesses of deposits on different samples (10<sup>16</sup> at./cm<sup>2</sup>). EPMA data

No	Element						
	B	Si	Cr	Fe	Ni	Cu	W
1	83	6	17	44	5	1	4
2	63	1	30	75	9	3	6
3	659	0	45	112	13	3	7
4	646	2	53	139	18	7	6
5	198	8	39	102	13	4	2
6	94	0	45	120	15	5	7
7	1	4	4	14	2	1	0
8	0	11	2	7	0.3	0	0
9	0	5	0.6	4	0.2	0	0

**Table 3.** D retention in samples 1-8

No	D concentration in deposit, at. %	Deposit thickness (RBS), 10 <sup>19</sup> at./cm <sup>2</sup>	D amount in deposit (NRA), 10 <sup>17</sup> D/cm <sup>2</sup>	D amount in sample (TDS), 10 <sup>17</sup> D/cm <sup>2</sup>
1	2	1.3	3.6	7.1
2	4	1.5	5.6	
3	5	1.9	7.9	
4	5	1.5	8.2	16
5	7	1.6	10	
6	8	1.4	12	
7	0	0	~0.001	0.32
8	0	0	~0.001	

Fig.1



Fig.2

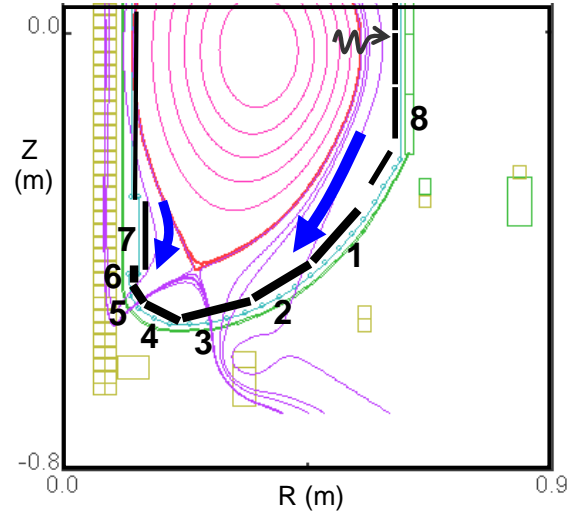


Fig.3

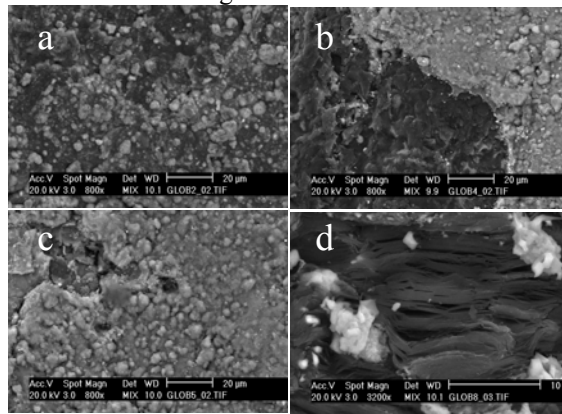


Fig.4

